JOURNAL OF MATERIALS SCIENCE: MATERIALS IN ELECTRONICS 8 (1997) 163–169

Photoluminescence studies of thermal impurity diffused porous silicon layers

K. B. SUNDARAM, S. A. ALI, R. E. PEALE*, W. A. McCLINTIC JR*
*Department of Electrical and Computer Engineering and * Department of Physics, University of Central Florida, Orlando FL 32816, USA*

Porous silicon layers were formed on diffused layers. Both boron and phosphorus impurities were thermally diffused using solid sources in n-Si, p-Si, n-epi/Si and p-epi/Si substrates of various resistivities. Porous silicon on these layers was formed by electrochemical and chemical etching under various etching conditions. Strong visible luminescence was observed from these porous silicon structures. Infrared absorption studies indicated that surface molecule identities are immaterial to the enhancement or degradation of photoluminescence.

1. Introduction

The first report of bright room-temperature photoluminescence (PL) from porous silicon (Po-Si) generated strong interest in the scientific community because it opened the door for consideration of silicon as a potential optical material which would be directly integrated to VLSI circuits [1]. Historically, Si has been the principal material utilized for integrated circuits, whereas III–V compounds such as GaAs or InP are extensively used in optoelectronics technology. However, compared to Si, there exist many problems with these III–V materials: the stability of the material, the quality of the oxide layer and the integrated reliability. Furthermore, the light emission from silicon is very inefficient, a consequence of its indirect bandgap structure.

The idea of integrating optoelectronic and conventional electronic devices on Si chips has been highly attractive due to the projected cost benefit, reliability and functionality. The increase in bandgap of porous silicon is due to the quantum confinement effects in these one-dimensional "wire-like" nanostructures [2, 3]. Room temperature PL has also been observed from quantized planar Ge and Si–Ge alloy layer structures [4, 5]. The porous silicon is obtained by a process of electrochemical anodization, which is much easier than quantum structure fabrication such as molecular beam epitaxy, plasma-assisted etching or microwave plasma decomposition. Hence special interest has been focused on porous silicon as a strong candidate for optical applications. However, in order to be useful as an optoelectronic material, porous silicon must provide bright electroluminescence (EL) not PL at useful wavelengths and with reasonable quantum efficiencies.

Electroluminescence from porous silicon was reported using liquid electrolyte solution as one of the electrical contacts; a luminescence efficiency of 0.1% was achieved [6]. However, applications to integrated circuits will require a solid-state EL device. Some solid-state EL devices were reported using porous silicon. Namavar *et al.* reported a heterojunction-based EL device using indium tin oxide (ITO) and porous silicon [7]. Electroluminescent devices using the structures Au/Po-Si/p-type Si/Al electrode were reported by other workers [8, 9]. Here the top Au layer was a thin transparent layer.

Visible electroluminescence was reported in n-type SiC/Po-Si/p-type structures [10]. The electroluminescence has been explained by a current injection mechanism [8, 11–13]. Ion-implanted p–n homojunctions have light-emitting properties [14]. But Po-Si obtained from ion-implanted layers has shown weak or no PL [15]. In order to make better p–n junction based Po-Si structures, it may be necessary to obtain Po-Si diffused layers by thermal diffusion.

Thermal diffusion can produce a relatively homogeneous doping with few defects. One does not want to carry out thermal diffusion of impurities in Po-Si after it is formed because the long high-temperature treatment quenches the PL intensity and shifts the peak energy wavelength [16]. Hence in this work, p–n junctions were first obtained by thermal diffusion, porous silicon layers were formed on these p–n junctions and the resulting structures were then studied.

2. Experimental procedure

In this experiment, one-side-polished p-type, n-type, n-epi/n^+, and p-epi/p^+ of various resistivities were used as substrate materials. The details are shown in Table I. The samples were cut into rectangular pieces of 1 cm × 4 cm. The cut pieces were cleaned by following the usual cleaning procedures adopted for silicon. After cleaning the wafers, approximately 1 μm of oxide was grown by a combination of wet and dry oxidation steps. Masking the back face of the sample with photoresist, the oxide on the front face

0957–4522

TABLE I Silicon samples used for experimental studies

Type	Orientation	Resistivity (Ω cm)	Thickness (μm)
n	(1 0 0)	3–4	250
n	(1 0 0)	50–100	500
p	(1 0 0)	8–15	300
p	(1 0 0)	17–23	500
n-epi/n^+	(1 0 0)	17–23	625/3.5 (epi)
n-epi/n^+	(1 0 0)	1.12–1.38	625/5.0 (epi)
p-epi/p^+	(1 0 0)	7–8	625/5 (epi)

was removed with hydrofluoric acid solution. The photoresist was then removed from the back face. Phosphorus and boron impurities were diffused into p-type and n-type substrates, respectively. The impurity diffusions were performed using solid-state sources and a two-step process involving a predeposition for 10–20 min at 950 °C followed by a drive-in diffusion at 1100 °C for durations in the range 20–30 mins.

Before the drive-in diffusion was performed, it was confirmed that type conversion of the diffused layer was achieved after predeposition. The sheet resistivities of the diffused layers were measured before and after drive-in diffusion steps. Boron diffusion calculations yielded junction depths in the range 1.16–1.63 μm for the n-type substrates that were used. Similar calculations yielded junction depths in the range 1.25–1.60 μm for phosphorus-diffused p-type substrates. Finally, the oxide was removed and aluminium was deposited on the back face. Annealing was performed in argon to get good ohmic contact on the back face. The back face was covered with photoresist or black wax and the front diffused layer was made porous by a chemical stain etch or an electrochemical etch.

The chemical stain etching was performed using two solution concentrations. They were 49% HF: 70%HNO_3:H_2O in the ratios 1:3:5 and 5:2:5 by volume. The etching durations were 3–10 min. n-Type layers were etched using light illumination. The stain etching was performed under room temperature conditions. The solution was stirred well during etching to make sure the bubbles produced were continuously

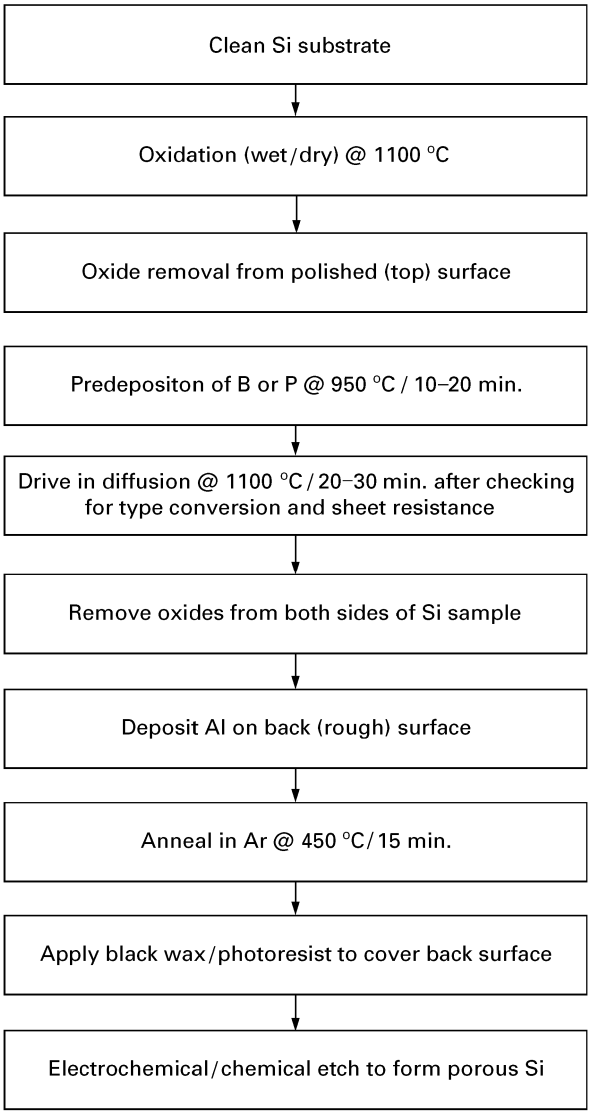

Figure 1 Process flow chart for the preparation of diffused porous Si samples.

removed. The electrochemical etching was performed in a solution containing 49%HF and ethanol (1:1 by volume) with current densities of 20–50 mA cm^{-2} for durations of 15–30 min. Light illumination was used for all the electrochemical etchings. The electrochemical etching was followed by an open-circuit etch in

TABLE II Chemically etched porous Si samples on diffused layers

Sample number	Type/ohm cm	Impurity diffused	HF:HNO_3:H_2O ratio	Integrated area (arb. units)	Peak wavelength (nm)
C2	n/3–4	boron	1:03:05	1.97E +05	617.28
D2	n/2–10	boron	1:03:05	1.90E +05	598.98
E2	n-epi/17–23	boron	5:02:05	7.05E +05	592.41
F2	n-epi/1.12–1.38	boron	1:03:05	1.58E +05	608.01
G2	n/60–80	boron	1:03:05	2.61E +05	610.31
H2	n/11–12	boron	1:03:05	1.14E +05	598.98
W2	p/8–15	phosphorus	1:03:05	2.23E +05	605.73
X2	p/17	phosphorus	1:03:05	2.01E +05	598.98
Y2	p/20	phosphorus	1:03:05	2.20E +05	590.24
KBS	p/8–15	undiffused	5:02:05	1.71E +05	619.65
227	p/8–15	undiffused	5:02:05	1.59E +05	601.21
D1 (electro-chemical etch)	n/2–10	boron	HF:ethanol (1:1)	1.01E +07	738.49

TABLE III Diffusion and etching conditions for the samples in Fig. 2

Sample	Diffusion conditions		Etching conditions		Integrated area	Peak wavelength (nm)
	Predep. time (min)	Drive-in time (min)	Current (mA)	Time (min)		
2a	20	30	50	30	0.461 E12	842
2b	20	30	50	15	0.203 E12	725
2c	18	30	50	15	0.964 E11	715
2d	12	30	50	15	0.925 E11	748
2e	10	30	20	30	0.858 E11	752

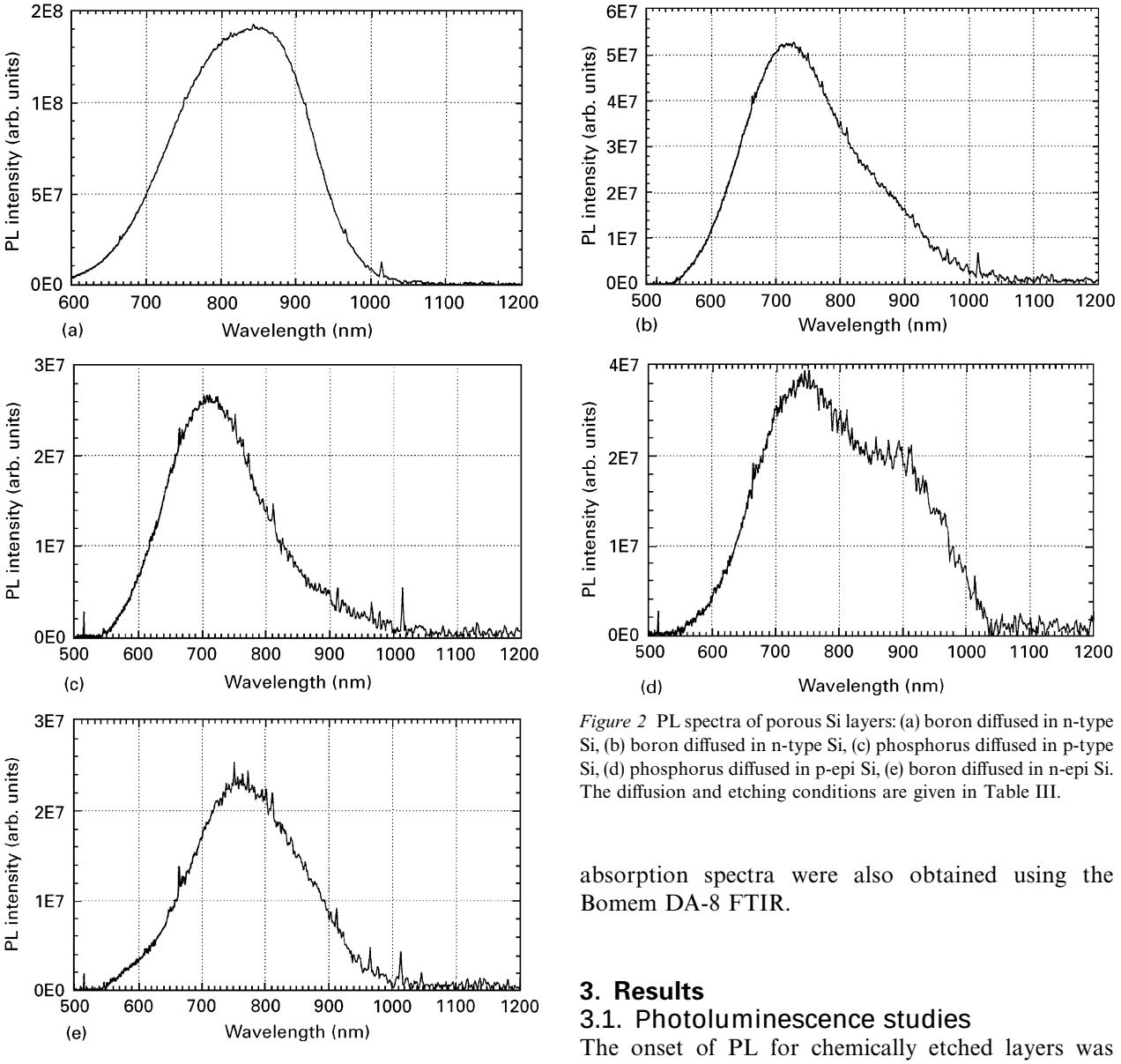

Figure 2 PL spectra of porous Si layers: (a) boron diffused in n-type Si, (b) boron diffused in n-type Si, (c) phosphorus diffused in p-type Si, (d) phosphorus diffused in p-epi Si, (e) boron diffused in n-epi Si. The diffusion and etching conditions are given in Table III.

a solution containing 49%HF and ethanol (1:3 by volume) for a period of 60 min to clean up any remaining oxide. The complete sample preparation sequence is shown in Fig. 1.

The PL tests were carried out by measuring the photoluminescence using a Bomem DA-8 Fourier spectrometer with an Si detector. The PL was excited using a CW 10 mW to 5 W multiline argon laser. The PL intensities were normalized and the integrated intensity areas were found for all the samples. The IR absorption spectra were also obtained using the Bomem DA-8 FTIR.

3. Results

3.1. Photoluminescence studies

The onset of PL for chemically etched layers was found by using a UV lamp (365 nm). An incubation period of around 3 min was required for PL to be observed. The PL studies on the chemically etched Po-Si layers showed weaker luminescence. Longer etching reduced the PL intensities considerably, even though a blue shift was observed. Table II shows the PL intensities of chemically etched Po-Si samples. For comparison, the intensity obtained for an electrochemically etched sample is also shown in the same table. The electrochemically etched sample has a much larger PL intensity than the chemically etched porous layer. Similar results were seen by Shih *et al.*

TABLE IV Electrochemically etched porous Si samples on diffused layers showing the effect of anodization time

Sample number	Type	Resistivity (Ω cm)	Impurity diffused	Diffusion data				Etch data		Normalized intensity (a.u)	Integrated area (a.u)	Peak wavelength (nm)
				Predeposition conditions		Drive-in conditions		Etch time (min)	Etch current (mA)			
				Time (min)	Sheet resistance ohm/square	Time (min)	ohm/square					
102	n	50–100	boron	10	140	20	350	15	50	3.14 E07	0.747 E11	735.1
111	n	50–100	boron	10	140	30	410	30	50	0.08 E07	0.337 E10	634.6
201	n	50–100	boron	10	190	20	642	15	20	1.75 E07	0.584 E11	728.5
220	n	50–100	boron	20	84	20	345	30	20	1.35 E07	0.238 E11	605.7
202	n	3–4	boron	10	190	20	642	15	50	4.55 E07	0.156 E12	770.1
221	n	3–4	boron	20	84	20	345	30	50	4.25 E07	0.143 E12	728.5
301	n-epi	1.1–1.4	boron	10	190	20	480	15	20	2.95 E06	0.137 E11	712.5
320	n-epi	1.1–1.4	boron	20	77	20	230	30	20	0.24 E07	0.278 E10	596.8
302	n-epi	1.1–1.4	boron	10	190	20	480	15	50	1.14 E07	0.375 E11	762.9
321	n-epi	1.1–1.4	boron	20	77	20	230	30	50	0.23 E07	0.762 E10	603.5
420	n-epi	8–15	boron	20	79	20	218	15	20	0.16 E07	0.321 E10	612.6
410	n-epi	8–15	boron	10	280	30	360	30	20	2.55 E06	0.545 E10	596.8
501	p	8–15	phosphorus	12	24.7	20	10.5	15	20	0.79 E07	0.250 E11	691.1
520	p	8–15	phosphorus	18	13.8	20	5.7	30	20	0.45 E07	0.166 E11	668.3
610	p-epi	7	phosphorus	12	22.3	30	9.1	15	20	5.12 E06	0.204 E11	804.6
601	p-epi	7	phosphorus	12	22.3	30	9.6	30	20	1.45 E06	0.281 E10	603.5

TABLE V Electrochemically etched porous Si samples on diffused layers showing the effect of anodization current

Sample number	Type	Resistivity (Ω cm)	Impurity diffused	Diffusion data				Etch data		Normalized intensity (a.u)	Integrated area (a.u)	Peak wavelength (nm)
				Predeposition conditions		Drive-in conditions		Etch time (min)	Etch current (mA)			
				Time (min)	Sheet resistance ohm/square	Time (min)	ohm/square					
101	n	50–100	boron	10	140	20	350	15	20	0.60 E07	0.208 E11	762.9
102	n	50–100	boron	10	140	20	350	15	50	3.14 E07	0.747 E11	735.1
130	n	50–100	boron	20	73	30	238	15	20	0.65 E07	0.192 E11	759.3
131	n	50–100	boron	20	73	30	238	15	50	5.25 E07	0.203 E12	725.3
210	n	3–4	boron	10	190	30	870	15	20	1.65 E07	0.531 E11	833.7
211	n	3–4	boron	10	190	30	870	15	50	0.42 E08	0.119 E12	738.5
320	n-epi	1.1–1.4	boron	20	77	20	230	30	20	0.24 E07	0.278 E10	596.8
321	n-epi	1.1–1.4	boron	20	77	20	230	30	50	0.23 E07	0.762 E10	603.5
430	n-epi	17–23	boron	20	79	30	250	15	20	0.18 E07	0.450 E10	601.2
431	n-epi	17–23	boron	20	79	30	250	15	50	0.53 E07	0.138 E11	951.4
501	p	8–15	phosphorus	12	24.7	20	10.5	15	20	0.79 E07	0.250 E11	691.1
502	p	8–15	phosphorus	12	24.7	20	10.5	15	50	0.19 E07	0.910 E11	688.2
530	p	8–15	phosphorus	18	13.8	30	5.4	15	20	2.24 E07	0.890 E11	735.1
531	p	8–15	phosphorus	18	13.8	30	5.4	15	50	2.67 E07	0.964 E11	715.6
610	p-epi	7	phosphorus	12	22.3	30	9.1	15	20	5.12 E06	0.204 E11	804.6
611	p-epi	7	phosphorus	12	22.3	30	9.1	15	50	3.42 E07	0.925 E11	748.7

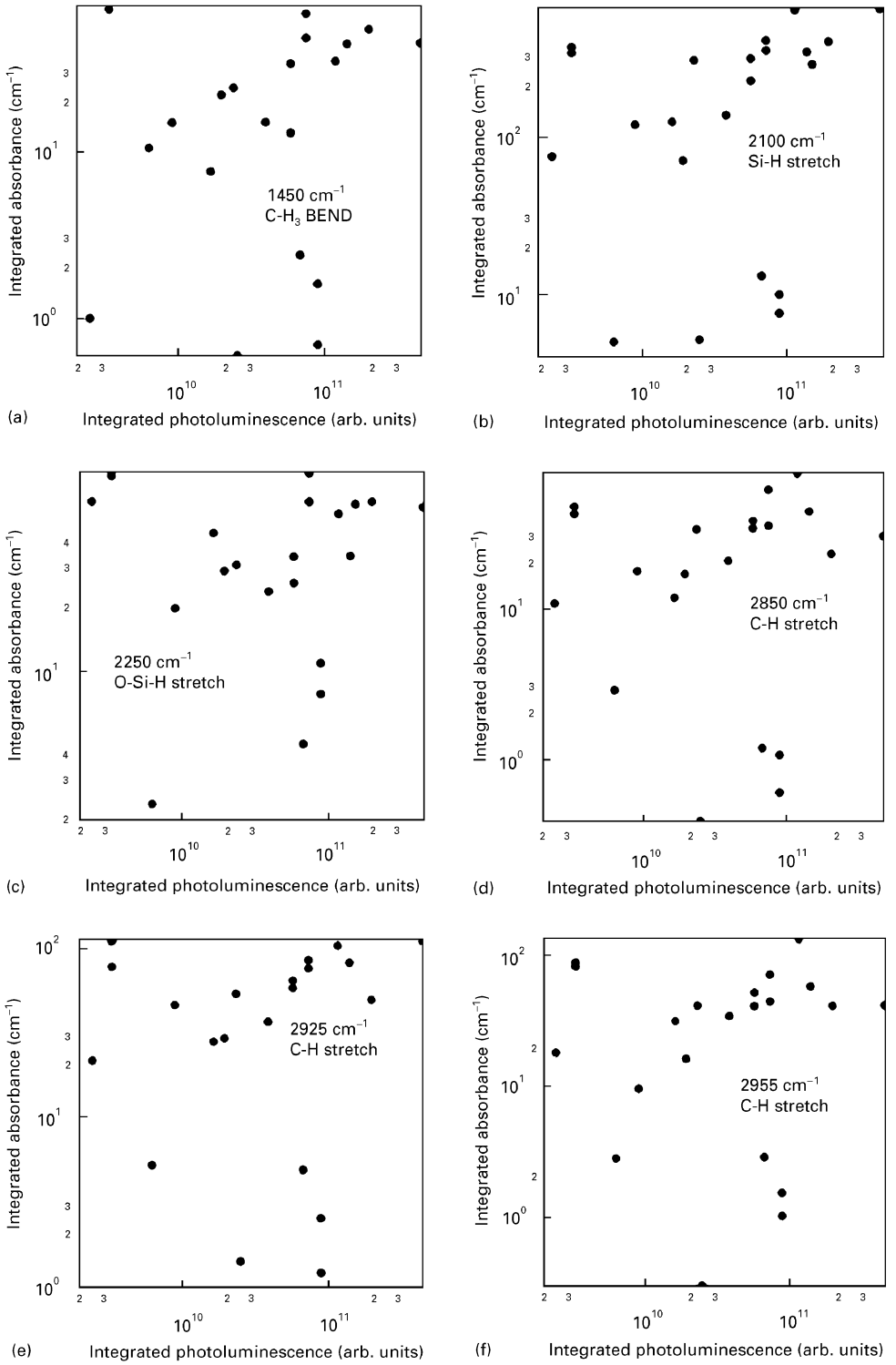

Figure 3 Integrated IR absorbance of various molecules versus porous Si integrated photoluminescence intensities.

for the stain-etched Po-Si on both n-type and p-type Si [17]. Values of the integrated intensity area for the porous layers prepared on diffused samples were in the same range as for the porous layers prepared on undiffused Si samples. The peak wavelengths were always shorter for chemically etched samples when compared with the electrochemically etched samples [17]. The peak wavelengths were in the range 590–620 nm for the chemically etched samples and did not vary much with process conditions. A similar trend was observed by Kiddler *et al.* for the Po-Si prepared on Si substrates [18].

Fig. 2 shows the typical PL spectra of porous layers obtained from various impurity-diffused samples on n-type, p-type, n-epi and p-epi Si substrates. Table IV summarizes the effect of etching time on the integrated intensity area and observed peak wavelength for a number of prepared samples. The etchings were performed for two durations, 15 and 30 min. All the conditions were kept constant for a pair of samples under investigation. Longer etching of the sample caused the integrated area of the intensity to decrease slightly and a tendency for the PL spectra to blue shift. Similar anodization time dependence on PL

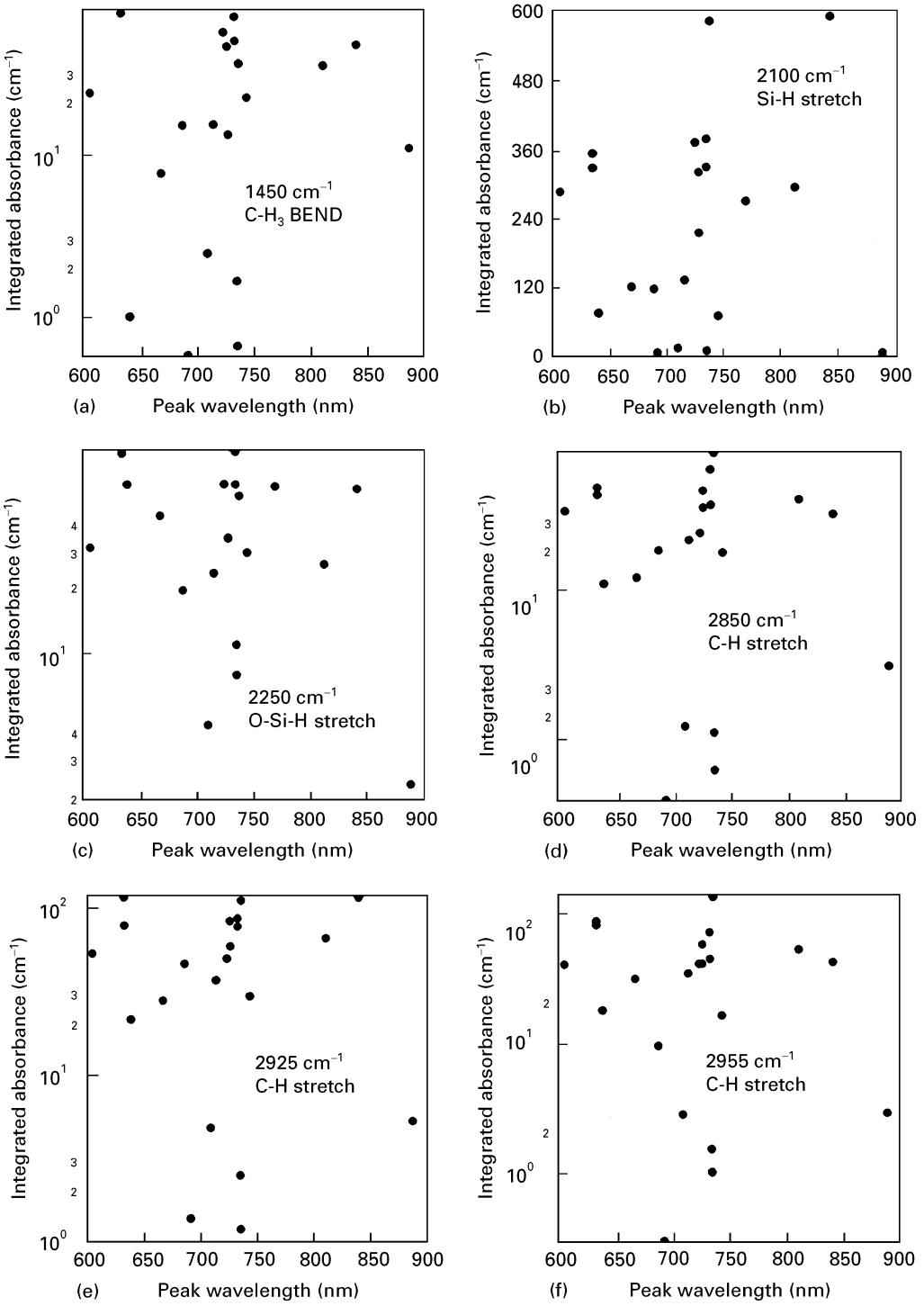

Figure 4 Integrated IR absorbance of various molecules versus porous Si peak photoluminescence wavelength.

wavelength was observed by Koshida and Koyama for the Po-Si samples prepared using Si [19]. Longer etching causes a reduction in the nanostructure size, thereby causing the blue shift. Table V summarizes the effect of anodization current on the integrated intensity area and peak wavelength for PL. Two current conditions were used, 20 and 50 mA. All other conditions were maintained constant for a pair of samples under investigation. The integrated intensity area increased for etchings performed at higher currents. The PL spectra showed a blue shift when the anodization current was increased. Similar results were seen by others for n-Si samples [19]. The samples prepared on n-epi substrates showed a tendency to red shift in PL spectra; this could not be understood.

3.2. Infrared absorption studies

Recent studies have correlated photoluminescence intensity with the infrared absorbance of specific molecules attached to the porous silicon surface. Some have observed a correlation between Si–H_n molecules

and PL strength, though this has been contradicted [20–23]. Others observe that absorption bands resulting from oxygen-related molecules are correlated with PL strength [24, 25]. And shifts in PL peak wavelength have been correlated with molecular infrared absorbance. Hydrocarbons have been correlated with a red shift [26]. An increase in oxide absorbance has been correlated with a blue shift [27]. Others observe no change in IR absorbance features when PL peaks shift after processing steps [28].

In our experiment the integrated infrared absorbance was measured for several lines and compared with the corresponding photoluminescence intensities and peak wavelengths; these comparisons are shown in Figs 3 and 4. All IR lines studied – they include oxides, hydrides, and hydrocarbons – appear uncorrelated with either PL intensity or peak wavelength. Our results support the view that surface molecule identities are immaterial to the enhancement or degradation of photoluminescence. Our experiments do not discount an alternative view that molecules on the surface control photoluminescence by passivating dangling bonds (non-radiative decay routes) and by adjusting quantum confinement through consumption of outer Si layers [29, 30].

4. Conclusion

Porous silicon prepared on diffused layers by chemical techniques or electrochemical etching showed good photoluminescence. Chemically stained layers showed a weaker PL intensity and a shorter PL spectral peak compared with electrochemically etched layers. IR absorbance studies on the porous Si layers indicated that the identity of the surface molecule is immaterial to the enhancement or degradation of photoluminescence.

References

1. L. T. CANHAM, *Appl. Phys. Lett.* **57** (1990) 1046.
2. A. G. CULLIS and L. T. CANHAM, *Nature* **353** (1991) 337.
3. R. BEHERNSMEIER, F. NAMAVAR, G. B. AMISOLA, F. A. OTTER and J. M. GALLIGAN, *Appl. Phys. Lett.* **62** (1993) 2408.
4. R. VENKATASUBRAMANIAN, D. P. MALTA, M. L. TIMMONS and J. A. HUTCHBY, *ibid.* **59** (1991) 1603.
5. A. KSENDZOV, R. W. FATHAUER, T. GEORGE, W. T. PIKE, R. P. VASQUEZ and A. P. TAYLOR, *ibid.* **63** (1993) 200.
6. L. T. CANHAM, W. Y. LEONG, M. I. J. BEALE, T. I. COX and L. TAYLOR, *ibid.* **61** (1992) 2563.
7. F. NAMAVAR, H. PAUL and N. KALKHORAN, *ibid.* **60** (1992) 2514.
8. N. KOSHIDA and H. KOYAMA, *ibid.* **6** (1992) 347.
9. A. RICHTER, P. STEINER, F. KOZLOWSKI and W. LANG, *IEEE Electron Lett.* **12** (1991) 691.
10. T. FUTAGI, T. MATSUMOTO, M. KATSUNO, Y. OHTA, H. MIMURA and K. KITAMURA, *Appl. Phys. Lett.* **63** (1993) 1209.
11. P. STEINER, F. KOZLOWSKI and W. LANG, *ibid.* **62** (1993) 2700.
12. H. P. MARUSKA, F. NAMAVAR and N. M. KALKHORAN, *ibid.* **61** (1992) 1338.
13. H. SHI, Y. ZHENG, Y. WANG and R. YUAN, *ibid.* **63** (1993) 770.
14. Z. CHEN and G. BOSMAN, *ibid.* **62** (1993) 708.
15. X. BAO and H. YANG, *ibid.* **63** (1993) 2246.
16. N. OOKUBO, H. ONO, Y. OCHIAI, Y. MOCHIZUKI and S. MATSUI, *ibid.* **61** (1992) 940.
17. S. SHIH, K. H. JUNG, T. Y. HSICH, J. SARATHY, J. C. CAMPBELL and D. L. KWONG, *ibid.* **60** (1992) 1863.
18. J. N. KIDDLER JR, P. S. WILLIAMS and T. P. PEARSALL, *ibid.* **61** (1992) 2896.
19. N. KOSHIDA and H. KOYAMA, *Nanotechnology* **3** (1992) 192.
20. C. TSAI, H. H. LI, J. SARATHY, S. SHIH, J. C. CAMPBELL, B. K. HANCE and J. M. WHITE, *Appl. Phys. Lett.* **59** (1991) 2814.
21. N. H. ZOUBIR, M. VERGNAT, T. DELATOUR, A. BURNEAU and P. DE DONATO, *ibid.* **65** (1994) 82.
22. J. M. LAVINE, S. P. SAWAN, Y. T. SHEIH and A. J. BELLEZZA, *ibid.* **62** (1993) 8.
23. P. D. STEVENS and R. GLOSSER, *J. Luminescence* **61/62** (1994) 383.
24. Y. H. SEO, H. J. LEE, H. I. JEON, D. H. OH, K. S. NAHM, Y. H. LEE, E. K. SUH and Y. G. KWANG, *Appl. Phys. Lett.* **62** (1993) 1812.
25. T. MARUYAMA and S. OHTANI, *ibid.* **65** (1994) 1346.
26. O. TESHCKE, F. GALEMBECK, M. C. GONCALVES and C. U. DAVANZO, *ibid.* **64** (1994) 3590.
27. S. L. ZHANG, F. M. HUANG, K. S. HO, L. JIA, C. L. YANG, J. J. LI, T. ZHU, Y. CHEN, S. M. CAI, A. FUJISHIMA and Z. F. LIU, *Phys. Rev. B* **51** (1995) 11194.
28. S. SHIH, K. H. JUNG, D. L. KWONG, M. KOVAR and J. M. WHITE, *Appl. Phys. Lett.* **62** (1993) 1904.
29. Z. CHEN and G. BOSMAN, *Phys. Status Solidi* (*b*) **184** (1994) 283.
30. X. WANG, P. HAO, D. HUANG, F. ZHANG, M. YANG and M. YU, *Phys. Rev. B* **50** (1994) 12230.

Received 15 April
and accepted 25 October 1996